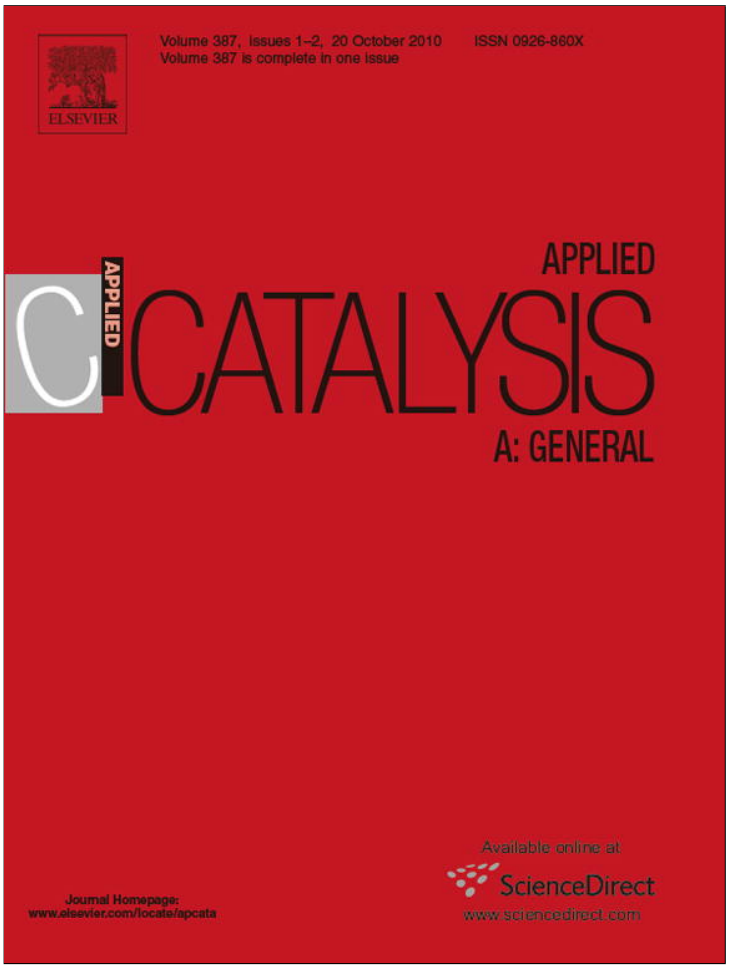

Applied Catalysis A: General 387 (2010) 35–44

Contents lists available at ScienceDirect

Applied Catalysis A: General

journal homepage: www.elsevier.com/locate/apcata

Screening of optimal pretreatment and reaction conditions for the isomerization-cracking of long paraffins over $Pt/WO_3–ZrO_2$ catalysts

M. Busto, J.M. Grau, C.R. Vera*

Instituto de Investigaciones en Catálisis y Petroquímica – INCAPE- (FIQ-UNL, CONICET), Santiago del Estero 2654, 3000 Santa Fe, Argentina

ARTICLE INFO

Article history:
Received 11 April 2010
Received in revised form 28 July 2010
Accepted 30 July 2010
Available online 14 August 2010

Keywords:
Tungsten–zirconia
Reaction conditions
Hexadecane
Cracking
Isomerization
Gasoline

ABSTRACT

Pretreatment and reaction conditions for the isomerization-cracking of long paraffins over commercial $Pt/WO_3–ZrO_2$ catalysts were screened. Optimal conditions were seeked for the production of short, high octane branched paraffins for the gasoline pool. *n*-C_{16} was used as a model molecule. The reaction over the acidic catalyst was used to adjust the size of the molecules to the boiling range of gasolines and to add branching in order to increase the octane number of the product. These adjustments had to be done while minimizing the production of light gases and getting a stable activity level.

With respect to the pretreatment it was confirmed that the best calcination temperature of the tungstate oxoanion promoted hydroxides was 800 °C. Optimality was mostly related to the activity level. The optimum temperature coincides with the appearance of small WO_3 crystallites which are thought to be center for creation of Brönsted acid sites in the presence of platinum and hydrogen.

Regarding the reaction conditions, increasing temperature values augmented the conversion but also increased the cracking. Therefore optimum values were found at moderate temperature given the high reactivity of the feed. Space velocity values were analyzed with attention to the liquid C_{5+} yield, the selectivity to branched isomers and the stability of the catalysts. Best yields to branched naphtha products were obtained with $Pt/WO_3–ZrO_2$ at WHSV = 18 h^{-1}. The catalyst coking rate was a function of the H_2/hydrocarbon ratio. A value of 6 was enough to attain a stable conversion value on $Pt/WO_3–ZrO_2$. The values of liquid yield as a function of pressure displayed a volcano pattern that was rationalized in terms of a non-classical bifunctional mechanism of reaction.

High pressure values increased the concentration of Brönsted acid sites and hence the activity. Too high pressures enhanced hydrocracking and decreased the liquid yield.

The results indicate that in general terms $Pt/WO_3–ZrO_2$ at moderate reaction conditions transforms a paraffinic heavy cut into a branched isomerizate that can be added to the gasoline pool to improve the quality properties. It was however found that under some conditions the octane gain is inversely proportional to the yield of light gases indicating that a high RON isomerizate can only be got at the expense of the liquid yield.

1. Introduction

Gasoline is a hydrocarbons mixture used as a fuel of motors of spark ignition. The composition of this mixture has greatly evolved in the last decades to accommodate two fundamental restrictions: (i) quality, mainly determined by the limit of minimum RON (Research Octane Number); (ii) toxicity, as measured by the set of values of concentration of compounds with noxious effects on the environment and the human life.

A virgin naphtha cut is composed of normal paraffins and naphthenes of five to eight carbon atoms and has an approximate RON value of 68 points. This value must be raised to 95–98 in order to satisfy the requirements of modern motors.

This article is devoted to the study of the transformations of long paraffins on a high acidity catalyst, $WO_3–ZrO_2$. In order to understand the necessary transformations long paraffins should undergo to become a high quality isomerizate some concepts about octane rating should be revised. Octane number measures the anti-knocking capacity of a fuel and depends on the chemical nature of its components. Some general trends can be deduced by analyzing large RON data sets, like those published by API [1]. Fig. 1 shows the variation of the RON of different chemical families: normal paraffins, isoparaffins, aromatics, naphthenes and olefins, as a function of their carbon number. Aromatic compounds display the highest RON, followed by naphthenes, olefins and isoparaffins. Normal paraffins have negligible RON. It can also be seen that for isoparaffins RON increases with the branching and for molecules of equal chemical nature (aromaticity, branching, substitution) it decreases with carbon number. It can also be deduced

* Corresponding author. Tel.: +54 342 4533858; fax: +54 342 4531068.

0926-860X/$ – see front matter © 2010 Elsevier B.V. All rights reserved.
doi:10.1016/j.apcata.2010.07.061

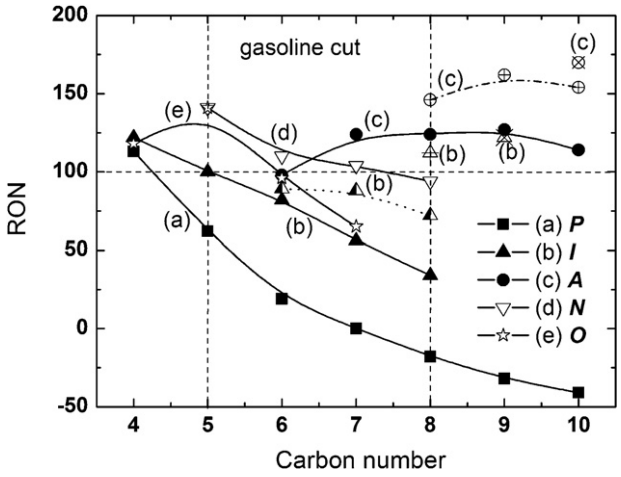

Fig. 1. RON of different chemical families as a function of the molecule carbon number. (a) Paraffins; (b) isoparaffins; (c) aromatics; (d) naphthenes; (e) olefins.

that RON is increased by the presence of tertiary and quaternary carbons.

According to the previous discussion and the insight of Fig. 1, isomerization-cracking of long paraffins should produce molecules in the C_5–C_8 range with the highest possible branching. From a thermodynamic point of view branching is a function of temperature and molecular size. Some long chain branched compounds, like 2,2,3-trimethyl-pentane have a high octane number (RON = 100) but they are in thermodynamic equilibrium with other isoparaffins of same carbon number and much lower RON. Therefore branched C_5–C_6 cuts are to be preferred to heavier cuts. The challenge to refiners is to maximize the quality and throughput of isomerizate while getting a stable operation and a minimum yield of light gases.

The most desirable features of the isomerizate are intimately linked to the choice of the catalyst. In this sense oxoanion promoted zirconia catalysts, Pt/SO_4^{2-}–ZrO_2 (Pt/SZ) and Pt/WO_3–ZrO_2 (Pt/WZ), have attracted the interest of researchers in the last decade due to their high activity at low temperatures. Catalysts based on Pt/SZ are indeed the base of the Par-Isom process (UOP) for isomerization of C_5–C_6 virgin naphtha.

A more recent and less studied application of oxoanion promoted zirconia catalysts has been the isomerization-cracking of long paraffins, Fischer–Tropsch waxes and plastics to produce short branched paraffins for the gasoline pool. In previous reports Pt and other noble metals (Ni, Pd, etc.) have been impregnated over SZ and WZ supports and their activity in isomerization-cracking of long paraffins has been assessed [2–5]. All reports conclude that Pt provides the most convenient metal function because it produces more active and stable catalysts. For this reason in this work only Pt/WZ catalysts are studied. Though many reports on the isomerization-cracking of long paraffins exist no single work focuses on the optimization of reaction conditions for obtaining a high RON isomerizate. Such focus is taken in this work.

Commercial WZ supports, a fixed content of Pt (0.5%) and a fixed Pt reduction temperature (300 °C) are used. All other pretreatment and reaction parameters are varied (activation temperature, reaction temperature, total pressure, H_2/hydrocarbon ratio).

Some studies on the hydrocracking of long paraffins are worth to be referenced. Deldari [6] studied the hydroisomerization of n-hexadecane over bifunctional catalysts, such as silica–aluminas, zeolites, tungsten and sulphate promoted zirconias and MCM-41 mesoporous materials. Wang et al. [7] studied modified and unmodified zeolites using dodecane as test molecule. Their results suggest that the catalysts with the highest concentration of Brönsted acid sites of medium strength are the most active in isomerization. Other works compare the activity and selectivity of Pt/WZ catalysts in the hydrocracking of n-hexadecane against other bifunctional catalysts based on USY zeolites and amorphous silica–alumina [8]. Walendziewski et al. [9] reported results of mechanical mixtures of zirconia catalysts (WZ and SZ) with alumina for the reaction of hydroisomerization and hydrocraking of waxes.

The only pretreatment variable studied in this work is the temperature of calcination of the support as this determines the total amount and the strength distribution of the acid sites. Its influence on the performance of the catalysts is specially studied because of its impact on the rates of isomerization and cracking.

2. Experimental

2.1. Catalysts preparation

A WO_3–ZrO_2 support with 15% W was supplied by MEL Chemicals in the form of a powdery hydroxide gel. This was first pressed into the form of pellets using a die and an hydraulic press. Then it was ground and sieved to 35–80 meshes. Several calcination treatments were performed in order to find the best temperature. The catalyst was calcined at 2 °C min^{-1} in air from room temperature to 180 °C and then this value was held for 1 h. Then the temperature was increased in h to the desired value (600, 700, 800 °C) and held for another 2 h. The sample was then cooled down to room temperature and unloaded. The obtained crystalline solid was then impregnated with chloroplatinic acid by the incipient wetness method. The amount of solution was regulated to obtained 0.5% Pt in the final catalyst. Once impregnated the sample was kept 24 h at room temperature and then dried slowly in a stove. The temperature was raised slowly from room temperature to 110 °C in order to prevent the solvent carrying over the metal precursor to the pore mouths. The dried material was then calcined in air in a muffle at 500 °C and cooled down in nitrogen. The metal phase was reduced by placing the sample in a hydrogen stream (30 cm^3 min^{-1} g^{-1}) and heating at 300 °C for 1 h. The thus obtained samples were called Pt/WZ_{T_c}, where T_c is the calcination temperature (in Celsius degrees).

2.2. Catalysts characterization

The physicochemical characterization of the catalyst was done using element chemical analysis, X-ray diffraction (crystallinity and crystal phase), nitrogen adsorption (specific surface area and pore volume distribution), pyridine adsorption (acidity) and n-hexane test batch reaction (activity, selectivity). The metal phase was studied by CO chemisorption and test reaction of cyclohexane dehydrogenation.

The chemical analysis of the Pt content of the solids was determined by atomic emission spectroscopy (ICP-AES) using an ARL model 3410 equipment. The solids were dissolved in a digestive pump with a mixture of 1 ml sulphuric acid, 3 ml chlorohydric acid and 1 ml nitric acid. The W content was determined by X-ray fluorescence.

X-ray diffraction spectra were measured in a Shimadzu XD-1 equipment with CuKα radiation filtered with Ni. The spectra were recorded in the 2θ range between 20° and 65° and with a scanning rate of 1.2 min^{-1}. The percentage of tetragonal phase of the samples was calculated using Eq. (1) [10]. The peaks located at $2\theta = 28°$ and $2\theta = 31°$ were attributed to the monoclinic phase of zirconia and those located at $2\theta = 30°$ to the tetragonal phase. The peaks located at $2\theta = 23$–$25°$ were attributed to WO_3 crystals.

$$X_t\ (\%) = \frac{100\,\alpha I_t}{I_m + \alpha I_t} \quad (1)$$

where X_t (%) = content of the tetragonal phase; $\alpha = 0.81$; I_t = integrated intensity corresponding to the (1 1 1) tetragonal peak; I_m = sum of the integrated intensities of the (1 1 1) and (1 1 −1) monoclinic peaks.

The quantification of the amount of each crystalline phase and the amount of amorphous matter was made by Rietveld Quantitative Analysis (RQA) [11–13]. From these values the crystallinity percentage was calculated. Calibration constants were computed from reliable structural data.

The physical properties of the catalysts were determined from nitrogen physisorption data. Nitrogen adsorption was performed in a Micromeritics 2100 E equipment. The specific surface area (S_g) was measured by the BET method with data of the adsorption branch of nitrogen at 77 K and the pore distribution by the BJH method with data of the desorption branch.

The acidity was measured by FTIR of adsorbed pyridine. The adsorption was performed in a glass equipment. The adsorbed amount was assessed by light absorption in the infrared region (1400–1600 cm^{-1} range). The measurements were performed in a Nicolet Avatar 3600 FTIR spectrometer. Self supported circular wafers (2 cm diameter, 50 mg) of the catalysts were used and they were vacuum treated in a cell with KCl windows. Residual pressure was less than 10^{-5} Torr.

Additional experiments of temperature programmed desorption of pyridine were also performed. 200 mg of the catalyst were first immersed in a closed vial containing pure pyridine (Merck, 99.9%) for 4 h. Then the catalyst was taken out from the vial and excess pyridine was removed by evaporation at room temperature under a fume hood. The sample was then charged to a quartz micro reactor and a constant nitrogen flow (40 $cm^3\,min^{-1}$) was established. Weakly adsorbed pyridine was first desorbed in a first stage of stabilization by heating the sample at 110 °C for 2 h. The temperature of the oven was then raised to 600 °C at a heating rate of 10 °C min^{-1}. The reactor outlet was directly connected to a flame ionization detector to measure the desorption rate of pyridine.

For CO chemisorption the experiments were performed in a chemisorption equipment designed ad hoc. The catalyst was placed in a quartz reactor, calcined 1 h at 500 °C in air flow and reduced in situ in a hydrogen stream (500 °C, 1 h, 60 $cm^3\,min^{-1}$). Then the carrier was switched to N_2 and the adsorbed hydrogen was desorbed (500 °C, 60 $cm^3\,min^{-1}$) for 1 h; then the cell was cooled down to room temperature. Then 0.25 cm^3 pulses of diluted CO (3.5% CO in N_2) were fed to the reactor. Non-chemisorbed CO was quantitatively transformed into CH_4 over a Ni/Kieselgur catalyst and detected in a flame ionization detector connected on-line.

2.3. Reaction tests

The screening of reaction conditions was performed using the test of isomerization-cracking of n-hexadecane. The catalytic properties of the metal function were also evaluated using the test reaction of cyclohexane dehydrogenation.

2.3.1. Cyclohexane dehydrogenation

The dehydrogenation of cyclohexane (CH) to benzene is a reaction that is insensitive to the structure of the metal active site and the activity is known to be strictly proportional to the number of surface active sites [14,15]. It was performed under the following conditions: catalyst mass = 0.1 g, 300 °C, 1 atm, molar ratio H_2/CH = 16, WHSV = 12.6. Cyclohexane was supplied by Merck (spectroscopy grade, 99.9% pure). The specified sulphur upper limit was 0.001%. A tubular quartz reactor was used that had an internal diameter of 10 mm.

2.3.2. n-Hexadecane test reaction

n-Hexadecane (99.9%) was supplied by Merck (Darmstadt, Germany). In the case of the screening of the pressure, calcination temperature and reaction temperature conditions, the experiments were performed in a stirred tank reactor. In this way temperature and mass transfer resistances were reduced and consumption of reactants was also reduced to a minimum. The temperature was varied in the 200–400 °C range and the total pressure in the 1–20 atm range. The reactor was an all AISI 304 stainless steel vessel, with 0.20 l total volume and a magnetic coupling between the motor and the stirrer. The reaction was carried out in semicontinuous mode. The gas flowed continuously while the pressure and flow were maintained in the desired values with the aid of a backpressure regulator and a needle valve, respectively. The liquid phase was charged and discharged in batch mode. The gas phase was continuously sampled and analyzed by an on-line Shimadzu GC-8A chromatograph equipped with a flame ionization detector and a 100 m, squalane coated capillary column. The liquid phase was sample at longer intervals and analyzed off-line in another Shimadzu GC-8A gas chromatograph equipped with a flame ionization detector and a 50 m Phenomenex CP Sil capillary column.

In each experiment 500 mg of catalyst were first reactivated at 500 °C in air for 1 h to eliminate adsorbed water and then they were reduced in hydrogen at 300 °C for 1 h. The steel reactor was dried in a stove at 110 °C overnight before charging the catalyst. After putting it in the reactor, 26 ml of n-hexadecane are added. The reactor is closed and tested for leaks under nitrogen pressure. Then it is purged with hydrogen and the pressure is raised to the setpoint value at room temperature. The reactor is then heated to the setpoint temperature and the stirring is begun (20 Hz). The reaction is continued until the required time has elapsed and then all connection valves are closed and the reactor is put in a cold water bath to quench the reaction.

The remaining reaction variables (space velocity, H_2/hydrocarbon ratio, etc.) were studied in a trickle-bed reactor (see Fig. 2). The hydrogen flowrate was controlled by a high pressure, mechanical Cole–Parmer mass flow controller. The total pressure was controlled by a Swagelok backpressure regulator. The liquid flowrate was controlled by an HPLC Cole–Parmer pump. A gas–liquid separator after the condenser and backpressure regulator was used to vent the gas and collect the liquid phase. The gas phase was continuously sampled and analyzed on-line while the liquid phase was samples and analyzed off-line.

From the gas chromatography compositional data the total conversion (X) and the yields to each reaction product (Y_i) were calculated on a carbon basis according to the formulae in the following lines. The conversion was defined as:

$$X = \frac{HC^i - HC^0}{HC^i} \tag{2}$$

where HC^i is the concentration of the fed hydrocarbon at the reactor inlet and HC^0 is the concentration of the non-reacted hydrocarbon at the reactor outlet. The selectivity to each product i was defined as:

$$S_i = \frac{\text{yield of } i}{X} = \frac{A_i \times f_i \times n_i}{M_i \left(\sum A_i \times f_i \times n_i / M_i\right) X} \times 100 \tag{3}$$

where A_i is the area of the chromatographic peak of product i, f_i is its response factor, n_i is the number of carbon atoms of i and M_i is its molecular weight. The RON of the products mixture was calculated using the method of Nikolaou et al. [16]. The RON gain (ΔRON) in the reforming reactor was calculated as the difference between the RON of the products mixture and the RON of n-hexadecane.

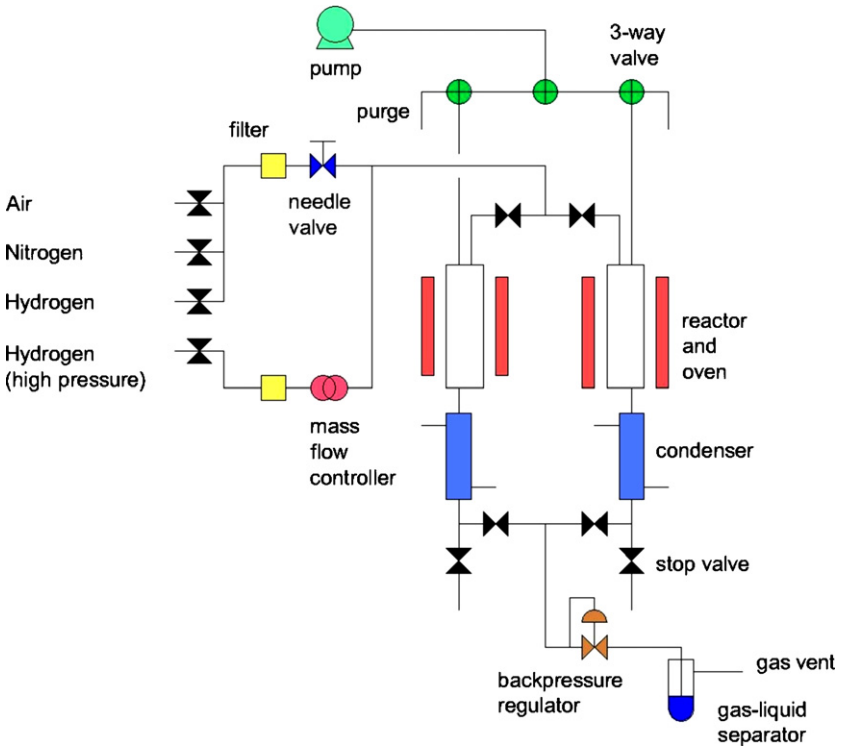

Fig. 2. Dual three-phase fixed bed reactor.

3. Results and discussion

3.1. Screening of calcination temperature

The chemical analysis confirmed that the percentage of Pt was not modified by the calcination treatment and that the real content lied within ±5% of the theoretical value calculated from the amount of precursor impregnated. The calcination treatment does not modify the W content either.

Table 1 shows the changes in the crystal and textural properties of the Pt/WZ catalyst calcined at different temperatures. On average the support has a final specific surface area of ~100 $m^2\,g^{-1}$ and a mean pore radius inside the mesopore range. When the calcination temperature is increased a decrease of the surface area can be seen. This is mainly due to the sintering of the micropores and hence a parallel increase of the pore radius is recorded. The sample calcined at 600 °C is totally tetragonal while in the others the percentage of tetragonality is slightly decreased when the calcination temperature is increased.

Fig. 3 shows the XRD spectra of the WZ catalysts calcined at different temperatures. The segregation of tungsten as WO_3 becomes evident at 800 °C. At this temperature peaks at $2\theta = 23.28°$, 23.78° and 24.48° appear [17]. It can be seen that a transformation of zirconia from the monoclinic to the tetragonal habitat occurs when the calcination temperature is increased to 800 °C.

Table 1
Physical properties of WO_3–ZrO_2 (WZ) calcined at different temperatures.

T_c [°C]	S_g [$m^2\,g^{-1}$]	D_p [nm]	V_p [$cm^3\,g^{-1}$]	T [%]
600	119.6	5.9	0.160	100.0
700	97.9	6.2	0.152	86.1
800	76.3	6.7	0.150	81.8

T_c: calcination temperature; S_g: BET specific surface area; D_p: mean pore diameter; V_p: pore volume; T: relative amount of tetragonal phase (%).

This transformation is accompanied by the growth of the WO_3 peaks. During calcination it has been reported [18] that many surface species are removed and that the process leads to the existence of both oxidized and reduced W atoms (W_{5+}, W_{6+}). This leads to the formation of anionic vacancies and the stabilization of the zirconia tetragonal habitat. When the samples are calcined at 800 °C many surface W_{5+} are oxidized to W_{6+} and the previous structure

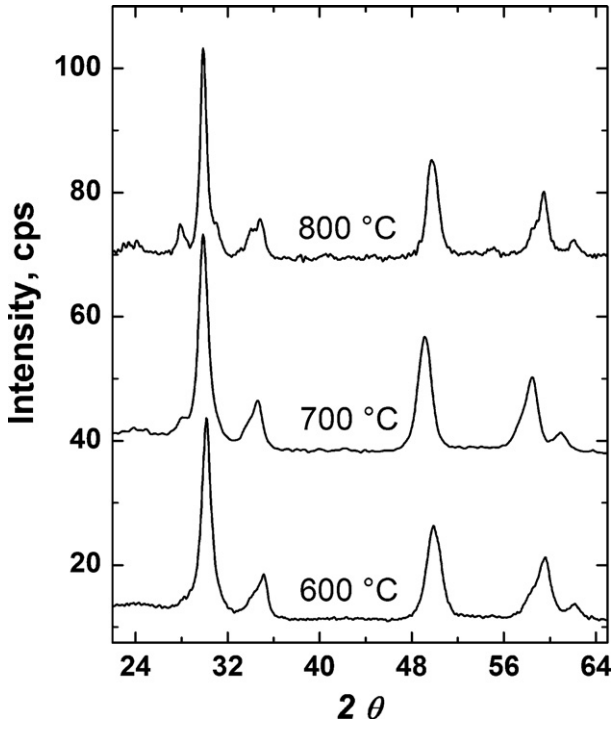

Fig. 3. X-ray diffraction results.

Table 2
Influence of the temperature of calcination of the support. Reaction conditions: T_R = 225 °C; t_R = 1 h; P_R = 10 atm; m_{cat} = 0.5 g; $m_{n\text{-}C_{16}}$ = 20 g.

T_c [°C]	X [%]	Y_{C1-C4} [%]	Y_{C5-C9} [%]	$Y_{C10-C15}$ [%]	$Y_{i\text{-}C16}$ [%]
600	69.9	0.0	6.9	5.8	57.2
700	62.1	0.0	1.7	1.1	59.2
800	85.6	0.1	5.3	6.3	73.9

T_c: temperature of calcination.

becomes unstable. As a result W sinters into bigger WO_3 particles and zirconia transforms to the monoclinic phase.

3.2. Tests in the batch reactor

These tests for selecting the temperature of calcination of the catalysts were performed with samples calcined at 600, 700 and 800 °C. The results are presented in Table 2. The total conversion is increased when augmenting the calcination temperature. There seems not to exist a correlation between textural properties such as specific surface area and content of tetragonal phase, with catalytic activity. Most likely activity is related to the amount and nature of acid sites. For this reason a detailed study of the surface acid sites was performed.

The results of FTIR spectroscopy of adsorbed pyridine can be seen in Fig. 4. This technique is useful for identifying Lewis and Brönsted acid sites. Pyridine tends to adsorb over aprotic catalytic sites (Lewis) or protic ones (Brönsted) through the free electronic pair of nitrogen and this step can be detected by the differential vibration of the ring. Pyridine adsorbed over WZ and SZ have characteristic bands in the 1400–1650 cm^{-1} range. Pyridine adsorption over Brönsted sites forms a pyridinium ion with bands at 1638, 1611 and 1540 cm^{-1} while the covalent bond of pyridine on Lewis

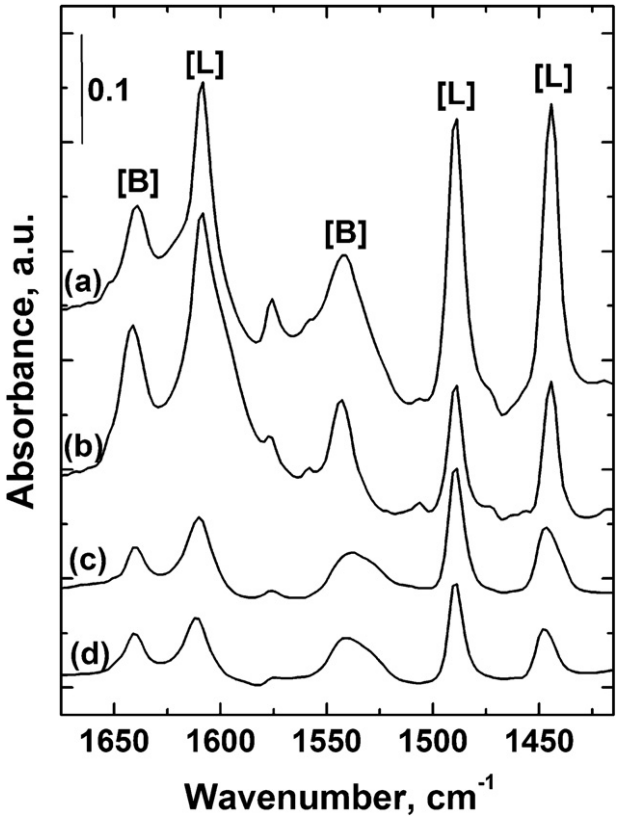

Fig. 4. FTIR spectrum of pyridine adsorbed on the catalyst. (a) Calcined at 600 °C; (b) calcined at 600 °C, reduced in H_2; (c) calcined at 800 °C; (d) calcined at 800 °C, reduced in H_2.

Table 3
Results of FTIR of pyridine adsorbed over the catalysts calcined at different temperatures, with and without reduction pretreatment.

	B/L		B/T	
T_c [°C]	600	800	600	800
WZ	0.42	0.65	0.3	0.4
WZred[a]	0.44	1.9	0.3	0.66

T_c: temperature of calcination; B/L: ratio of the intensity of the bands due to Brönsted and Lewis acid sites; B/T: ratio of the intensity of the bands due to Brönsted acid sites and total acid sites.

[a] Catalysts reduced in hydrogen at 300 °C before adsorbing pyridine.

acid sites has characteristic bands at 1607, 1486 and 1445 cm^{-1} [19–21].

In Table 3 we can see the values of the intensity of the bands of pyridine adsorbed only on Brönsted sites, only on Lewis sites and on any of them. The FTIR spectra of pyridine adsorbed over WZ show that when the calcination temperature is increased the Brönsted/Lewis ratio is decreased. This can be correlated with the activity results. The concentration of Brönsted acid sites decreases with the increase in the calcination temperature. However this does not correlate with the catalytic activity results. The results can however be explained by the transformations occurring on the surface in the presence of hydrogen [22–25]. This includes not only the reduction of the metals (Pt and W) during pretreatment and reaction. This is seen in the FTIR results corresponding to the previously reduced WZ catalysts. Reduction in hydrogen at 300 °C before the adsorption of pyridine clearly increases the Brönsted/Lewis ratio, indicating that Brönsted acid sites are formed by the reduction treatment. Similar results have been reported by Shimizu et al. [26] and they have been attributed to the transformation of Lewis into Brönsted sites. Other authors [27] have in situ measured the amount of Brönsted acid sites (by titration of 2,6-di-tert-butilpiridina) and reduced centers (by UV–Vis spectroscopy) with the objective of elucidating the way these species were formed and what role they had in the dehydration of 2-butanol. Using 2-butanol as stoichiometric reducing agent $H_{\delta+}(WO_3)n_{\delta-}$ sites are formed that are catalytically active. In these sites the charge is stabilized over many W atoms with low degree of reduction.

Barton et al. [28] made a similar analysis for the isomerization of o-xylene over Pt/WZ and they found that the catalytic activity is strongly influenced by the surface density of WO_x. They used hydrogen in the reaction of o-xylene over WO_3–ZrO_2 in order to generate and keep a stable concentration of Brönsted $H_{\delta+}(WO_3)n_{\delta-}$ sites. It can be seen from these findings that the measurement of the concentration of Brönsted acid sites must be done at reaction conditions in order to precisely determine the sites present in the reaction.

In summary it can be concluded that the catalytic activity of Pt/WZ is related to the presence of Brönsted acid sites. To maximize the concentration of these sites the temperature of calcination of the support must be 800 °C.

The metal function supported on WZ previously calcined at 800 °C was characterized by means of the cyclohexane dehydrogenation reaction and the dispersion of the metal particles was measured by CO pulse chemisorption. For a cyclohexane conversion of 12.3% the selectivities to methylcyclopentane and benzene were 33% and 66.7%, respectively. These results indicate that there is a strong interaction of Pt with surface oxygen species. The interaction decreases the ability of Pt to dehydrogenate cyclohexane. The presence of methylcyclopentane among the reaction products indicates that both isomerization and dehydrogenation occur. Isomerization is related to the strong acidity of the support. The value of dispersion of the metal particles as measured by CO chemisorption was 73%. This value was expected because it is known that acidic tungsten–zirconia stabilizes small metal particles.

3.3. Reaction temperature

In order to see the reproducibility of the catalytic assays a series of 6 experiments was performed with the stirred tank reactor using the same catalyst and keeping constant the operation conditions (200 °C, time-on-stream = 1 h, 10 atm total pressure, 0.5 g of catalys, 20 g of *n*-C_{16}). The results varied as follows. Conversion: 37.3–42.8%, yield of C_{5-9}: 0.08–0.12%, yield of C_{10-15}: 0.58–1.94, yield of C_{16} isomers: 31.94–39.74%, yield of gases: 0.03–0.11%.

When screening the reaction temperature the other variables were kept in the same values used in the previous paragraph. The products were lumped into the following cuts: light gases (C_1–C_4), naphtha (C_5–C_8, NBP = 25–170 °C), kerosene (C_8–C_{15}, NBP = 170–225 °C) and hexadecane isomers (*i*-C_{16}). The range of products is determined by their retention time after calibration with known standards.

Fig. 5 shows the results of the n-hexadecane reaction over the Pt/WZ catalyst at different temperatures in the 200–300 °C range. At low temperatures there is a marked difference between the high yield to hexadecane isomers (45–50%) and the low yield to gases (<1%). When the reaction temperature is increased an important drop in the yield to hexadecane isomers occurs while there is a big increase of the yield to cracking products. The highest increase occurs in the naphtha fraction, indicating that cracking mainly occurs in middle positions of the molecule.

The analysis of figure indicate that in order to perform skeletal branching with low cracking (<1%) the best option is to use Pt/WZ at a reaction temperature of 200–225 °C because it has a high conversion (46–50%) and a selectivity almost complete to isomerization products. Temperatures outside the 225–250 °C range seem not attractive. At temperatures lower than 225 °C the acid activity of both catalysts is too low and the system is inhibited by the high activation energy needed for the isomerization over Pt/WZ. At temperatures higher than 250 °C there is an excessive cracking of the long paraffins. A temperature of 225 °C seems the most attractive.

3.4. Total pressure

Assays were performed varying the total pressure and using a temperature of 225 °C. The effect from the kinetic point of view is that of increasing the hydrogen partial pressure because hydrogen is the major component of the gas phase and this stream is only diluted by a small proportion of light gases formed.

On Pt/WZ (Fig. 6) an increase of the total pressure produces an increase of the conversion. The yield to hexadecane isomers is also increased, while the yields to gases, naphtha and kerosene remain low. This indicates that at the reaction conditions chosen the cracking rate is inhibited by the increase of the total pressure. When discussed in terms of a classical bifunctional mechanism, this variation has no explanation, because at a fixed H_2/*n*-C_{16} ratio the isomerization rate should remain constant or decrease [29]. If the results are however analyzed with the concepts of the non-classical bifunctional mechanism it can be rationalized that the higher hydrogen partial pressure favourably affects the rate of hydride transfer that is the final elementary step of this isomerization mechanism. Another possibility is that the higher partial pressure of hydrogen increases the concentration of dynamic Brönsted sites while the concentration of strong Lewis sites responsible for coking and cracking, is decreased. It must be recalled that the dynamic Brönsted sites are formed over Pt/WZ by reduction of strong Lewis acid sites. The range 15–20 atm is therefore optimum because both the conversion and the yield to branched isomers are maximized. The maximum conversion is obtained at 20 atm while the maximum yield to gasolines is obtained at 15 atm.

At this point some mechanistic issues should be discussed. For paraffinic feeds the reported order of reaction of hydrocracking is negative with respect to hydrogen. This is valid when the reacting system follows the classic bifunctional mechanism, in which the rate controlling step is the alkane isomerization. In this case when the hydrogen pressure is increased the thermodynamic equilibrium becomes non-favourable for the olefinic intermediate that migrates between acid and metal sites.

In Ref. [30] Parera et al. presented a non-classical bifunctional mechanism. The differences with the classical mechanism are obvious. At high temperatures only the classical bifunctional mechanism occurs because the formation of the intermediate olefins is possible and the main function of the metal is to produce olefins that can react over any acid site, even of low acidity. At low temperatures and over strong acidic oxoanion promoted zirconia catalysts the formation of olefins on the metal sites is not possible and hence the main function of the metal is the dissociation of hydrogen to produce new dynamic acid sites and to hydrogenate coke precursors.

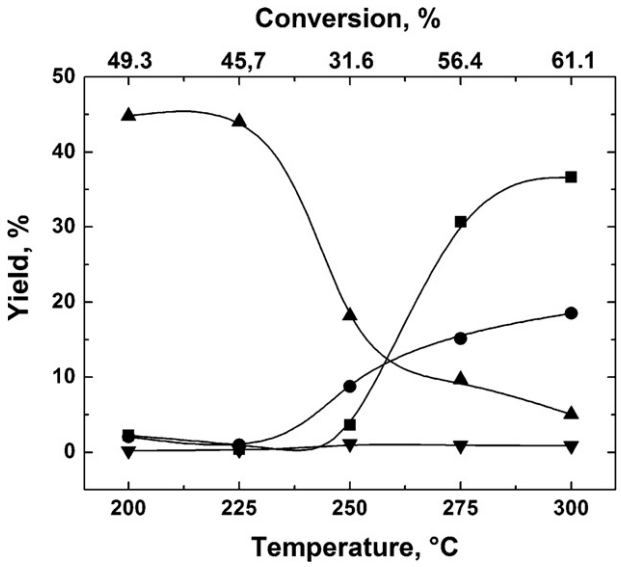

Fig. 5. Conversion and product yield as a function of the reaction temperature. TOS = 180 min; (Δ) isomers of hexadecane; (■) naphtha; (○) kerosene; (▼) gases.

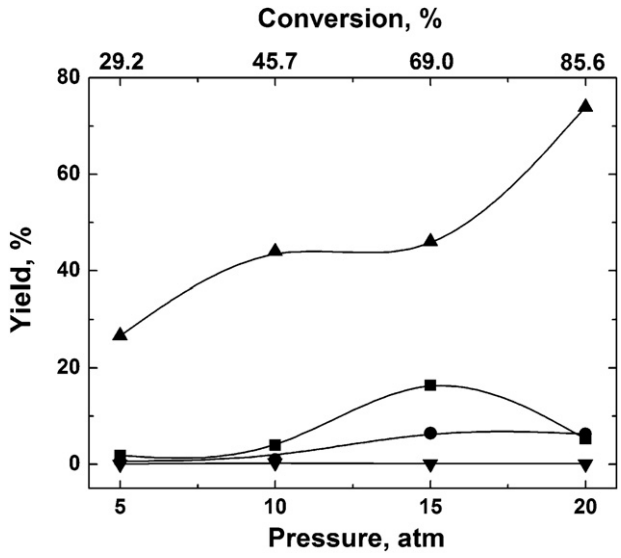

Fig. 6. Influence of the pressure on the product yield. Time-on-stream = 180 min; (Δ) *i*-C_{16}; (■) naphtha; (○) kerosene; (▼) gases.

Iglesia et al. [31] suggest that during the conversion of n-heptane at 200 °C isomerization occurs by direct reaction of the alkanes on the acid sites with the help of metal sites. Pt converts molecular hydrogen into activated hydrogen that diffuses on the catalyst surface and is transferred to the carbenium ion adsorbed on the acid site. This would explain the positive effect of hydrogen. Comelli et al. [32] studied the reaction of n-hexane at 200 °C and observed a positive effect of H_2 that was explained by the fact that hydrogen inhibits the deactivation of the catalyst and that hydrogen also shortens the half life of adsorbed carbocations. Duchet et al. [33,34] worked with n-hexane at 150 °C and observed a positive effect of the pressure increase from 760 to 4000 Torr. They suppose that bifunctional mechanism is unlikely to occur. They suggest a mechanism that involves Lewis sites. The abstraction of hydrides from the n-hexane molecules on the catalyst surface creates carbenium ions that get adsorbed over Lewis sites. The ion would be rapidly isomerized and finally desorbed as a paraffin after hydride transfer takes place. These hydrides are produced by homolytic dissociation of the hydrogen molecule on Pt atoms. Electronic transfers on the catalyst surface would also generate (Zr–H–)– and (O–H+). In this way the increment of the hydrogen pressure would increase the concentration of surface hydrides thus accelerating the desorption of carbenium ions and the global reaction rate. This idea can be better understood analyzing the non-classical bifunctional mechanism mentioned before. Hattori et al. [35–37] use this mechanism and suggest that molecular hydrogen is a source of Brönsted acidity. Molecular hydrogen is dissociated over Pt into hydrogen atoms that spillover to acid sites were they are converted into H+ and H−. According to these authors the contribution of the classical bifunctional mechanism would be negligible.

A last issue to analyze is that of the inhibition of the thus discussed pressure effect when the pressure is higher than 15 atm. A similar effect has been reported by Busto et al. [29] during the isomerization of n-hexane. According to this reference at high pressures there would be a competition of hydrogen for adsorption sites on the surface, thus competing with cyclohexane and reducing the population of adsorbed carbenium ions.

In summary in the interval studied the highest isomerization activity of Pt/WZ and the highest cracking activity of Pt/SZ occur both at 20 atm and this pressure value will be used for the rest of the study.

3.5. Partial pressure of hydrocarbon and hydrogen

After discussing the influence of total pressure a word should be said about the partial pressures of the hydrocarbon and hydrogen. In most reports the influence of the hydrocarbon partial pressure played a second role and the role of the hydrogen pressure was highlighted and much more studied. Deldari [6] made a comprehensive review on the hydroisomerization of long paraffins C_8–C_{16} and included Pt/WO_3–ZrO_2 and Pt/SO_4^{2-}–ZrO_2 in his report. The influence of the pressure was not discussed but the mechanism of hydroisomerization was supposed to be the classical bifunctional one, with olefinic intermediates. In this mechanism the skeletal rearrangement of the adsorbed carbenium ion is supposed to be the slowest step and the expression for the isomerization rate takes the form: $k\,p_{HC}/(K_1\,p_{HC} + K_2\,p_{H_2})$ [29,38]. The main term in the numerator is first-order in the hydrocarbon partial pressure (HC) while the numerator takes into account the effects of hydrocarbon and hydrogen adsorption. A similar equation, first-order in hydrocarbon pressure but with a different denominator, was elucidated by Duchet et al. [33,34] for the n-hexane isomerization on Pt/SO_4^{2-}–ZrO_2, assuming that hydride transfer to the adsorbed carbenium ions was the slowest step and that hydrogen was heterolytically dissociated on the surface. This assumption is in accord with previous suggestions of Iglesia et al. [31] that n-alkane isomerization on Pt/SZ proceeds via chain processes limited by hydride transfer steps which complete a surface turnover by desorbing carbenium ion intermediates.

In summary the isomerization rate has a positive order with respect to the hydrocarbon partial pressure though isomerization in the adsorbed state does not seem to be the rate-limiting step. The cracking rate has also a positive order with respect to the hydrocarbon pressure but in this case the cracking step depends primarily on the concentration of intermediate branched isomers [39]. Both rates are first favoured by the hydrogen pressure and then inhibited at increasing values, thus displaying similar volcano patterns, though cracking is more affected [40]. These reported results are in accord with our results for the naphtha yield as a function of total pressure of Fig. 6. This is not surprising because the values of the hydrogen-to-hydrocarbon ratio are usually much greater than one and then the patterns of activity as a function of total pressure mimick those of activity as a function of hydrogen partial pressure. The role of the partial pressure of the hydrocarbon in these plots is to shift the position of the volcano peak to the right at higher values of hydrocarbon pressure. This can be explained by considering that hydride transfer is the key step of the mechanism [40].

As expected, when increasing the molecular weight there is also an increase of the reaction rate and a modification of the products distribution. The global reaction rate is however decreased at high values of time-on-stream because of coking. Again here the partial pressure of hydrogen strongly determines the stable value of conversion because it regulates the rate of hydrogenation of coke precursors. This point will be revisited when considering the influence of the hydrogen-to-hydrocarbon ratio.

3.6. Tests in the fixed bed reactor

In this work values of the Reynolds number of the liquid phase were calculated as 3.9–7.7 and Reynolds numbers of the gas phase were 0.4–2.1. According to known correlations and maps of flow patterns the prevailing pattern in our experiments in the three-phase fixed bed reactor was therefore “trickling” [41,42].

With respect to the wetting efficiency the incomplete wetting in trickle-bed reactors has two causes [43]. The first is the bad distribution of the liquid phase in the reactor, thus leaving one portion poorly irrigated. This is solved with an adequate design of the distributor. As the incomplete wetting is related to a low liquid velocity the wetting can be improved by increasing the liquid flow rate. Also the gas flow rate and the pressure improve the wetting because they increase the tension in the gas–liquid interphase [44]. The second cause is the increment of the temperature in the reactor because of exothermal reactions taking place. The wetting degree has a great effect on the achieved conversion and can condition the operation of the reactor. If the limiting reactant is in the liquid phase then the complete wetting increases the conversion. If the limiting reactant is in the gas phase then an incomplete wetting will give higher conversion values [45]. Two ways of increasing the wetting efficiency are commonly used: (i) operating the reactor in upflow mode and (ii) operating in downflow mode with a bed of catalyst diluted with inert particles [46,47]. The experiments in this section and the next ones were performed with all reactants in downflow in order to avoid the flooding of the catalyst bed and to preserve the trickling pattern. The bed was diluted with particles of silicon carbide of 20–35 mesh that were previously calcined at 500 °C for 3 h. It was verified that the solid diluent is chemically inert at the reaction conditions. The wetting in all tests was assumed to be complete.

The importance of mass transfer resistances in the trickle-bed reactor was assessed by means of known correlations. The Weisz–Prater module was calculated from measured experimental values and was found to be much lower than 1. To reassure

Table 4
Reaction tests with different catalyst particle sizes.

	1	2		3	
Particle diameter [mesh]	>2	8–16		35–80	
Recorded reaction rate [mol h^{-1}]	0.0013	0.0159		0.0143	
Particle diameter [cm]	1.210	0.238	0.120	0.050	0.018
Φ, Weisz–Prater module	10.00	4.94	1.20	0.19	0.03

the convenience of the experimental conditions tests were performed with varying particle radius. These results are depicted in Table 4.

It can be seen that for particles smaller than 16 meshes practically no diffusive limitations exist. With respect to the axial dispersion we have indicated in a previous contribution [48] that conversion values can be decreased by the backmixing in tubular reactors with high values of axial dispersion. This dispersion is predicted by many published correlations [47–50]. Using the correlation of Michell and Furzer [50] a value of the Péclet number of 2 is obtained at all conditions. As a result to eliminate backmixing the length-to-particle diameter ratio should be equal to 50 or higher. The diameter of the reactor and the amount of diluent were adjusted to meet this criterion.

3.7. Space velocity

The effect of the space velocity (WHSV) on conversion and yield is depicted in Fig. 7. Values of residence time (1/WHSV) between 0.25 and 0.028 h were used. The other operation conditions were 225 °C, 20 atm and H_2/HC = 6. The conversion values are close to 97% except for the test at the lowest residence time, 0.25 h, for which the conversion drops to a value of 47.8%. At high residence time values the yield to gases reaches a value of 45% while it drops at lower values of the residence time. The fraction of the obtained naphtha (C_5–C_9) increases at low residence time values and reaches a maximum at 0.55 h. Both the yield to hexadecane isomers and the yield to kerosene do not reach 5%.

In Fig. 8 we can see the distribution by carbon number of the reaction products. When the residence time is increased the distribution becomes flatter and wider and the center is displaced to higher carbon numbers. In order to see the contribution of each carbon number fraction to the RON of the product Fig. 9 was plotted. It is a distribution of liquid C_5 + branched isomers as a function of carbon number. The distribution has a maximum at CN = 5 and CN = 7. From the point of view of the octane number for the same degree of branching the highest RON isomers are those of 5–6 carbon atoms. On a molar basis it is found that longer isomers decrease the relative volatility and increase the heat content. An optimal isomerizate naphtha would be one with 5–8 carbon atoms. If we recall Fig. 6 when the space velocity is the highest (lowest residence time) the products mixture has an excessive concentration of long molecules and the degree of branching at all carbon numbers is small. Conversely when the residence time is the highest the production of gases, specially isobutane, is maximum. In this case the low liquid yield makes this distribution unconvenient.

A space velocity of 18.4 h^{-1} produces the distribution with the richest iso-C_{5-8} fraction. In this case the liquid yield and the RON of the liquid fraction are maximum.

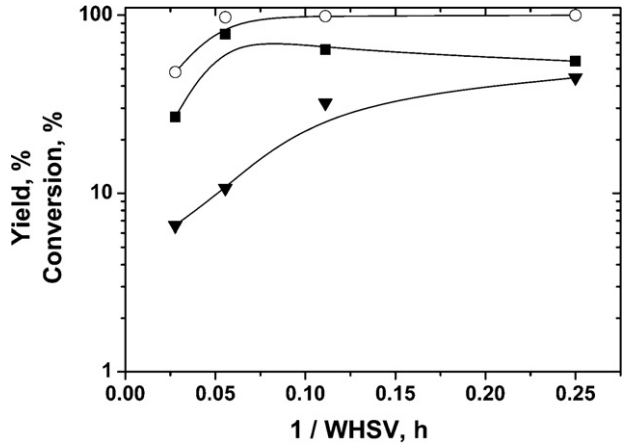

Fig. 7. Influence of the spatial velocity on conversion and product yield. Time-on-stream = 60 min; (○) conversion; (■) naphtha; (▼) gases.

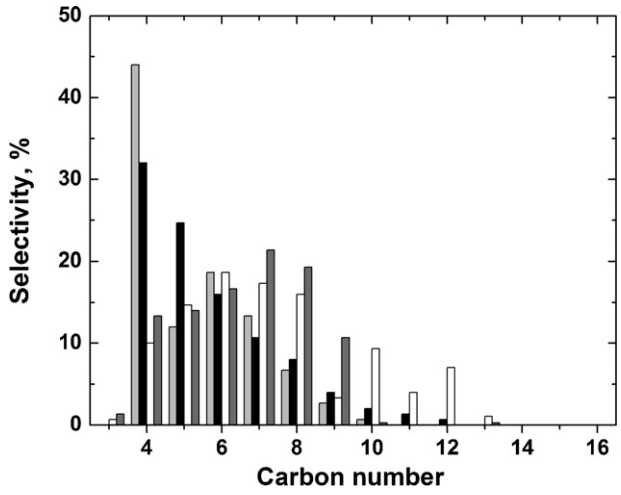

Fig. 8. Selectivity to all products of different carbon number. Time-on-stream = 60 min; ( ) WHSV: 4 h^{-1}; (■) WHSV: 9 h^{-1}; (□) WHSV: 18.4 h^{-1}; ( ) WHSV: 36 h^{-1}.

3.8. H_2/n-C_{16} molar ratio

The reason for varying this ratio is to find in which range the operation of the catalyst is stable. From an economic and process point of view a high H_2/HC ratio is costly because it dilutes the reacting mixture and reduces the total isomerizate throughput and mainly because it forces refiners to recycle great amounts of hydrogen. Molar ratios of 1 or lower, like those used in the Penex process, for example, enable a hydrogen once-through operation with great economies in operating costs. Fig. 10 contains data for different val-

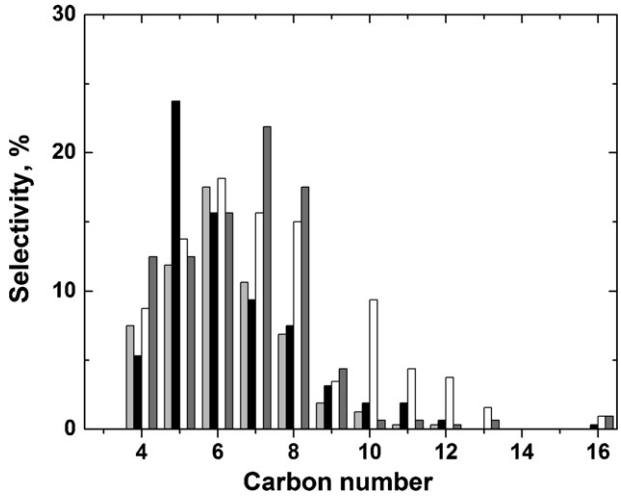

Fig. 9. Selectivity to branched products of different carbon number. Time-on-stream = 60 min; ( ) WHSV: 4 h^{-1}; (■) WHSV: 9 h^{-1}; (□) WHSV: 18.4 h^{-1}; ( ) WHSV: 36 h^{-1}.

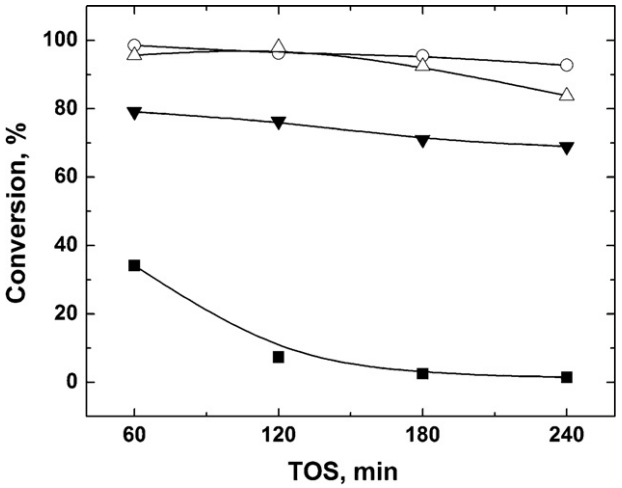

Fig. 10. Conversion as a function of time-on-stream for different values of the H_2/n-C_{16} ratio. (■) H_2/n-C_{16}: 0.5; (○) H_2/n-C_{16}: 6; (△) H_2/n-C_{16}: 10; (▼) H_2/n-C_{16}: 15.

ues of H_2/n-C_{16}, 0.5, 6, 10 and 15. The rest of reaction conditions are 225 °C, 20 atm, WHSV = 18.4 h^{-1}.

In the case of the Pt/WZ catalyst, molar ratios of 6 and 10 make the activity after 4 h reaction time to remain practically constant. Then it can be considered that H_2/HC = 6 is the optimum value for this variable. Probably lower values exist for which the catalyst is still stable. For the value of 0.5, the initial conversion is lower than those observed at other H_2/HC values and it drops to negligible values probably because of the formation of carbon deposits on the catalyst surface. On the other side the lower initial and final activities must be surely due to a lower concentration of Brönsted acid sites generated by spiltover hydrogen reduced on Lewis acid sites.

3.9. RON gain versus yield of light gases

A final analysis of the results was made by plotting the gain in octane points of the isomerizate as a function of the yield of light gases. This was done for all of the experimental points obtained in the work. The results can be found in Fig. 11. The sets of points are grouped taking into account the free variable. It can be seen that when the spatial velocity (WHSV) and the hydrogen-to-hydrocarbon ratio (H_2/HC) are varied a seemingly linear correlation exists between the RON gain and the yield to light gases. The practical consequences of this is that under these conditions an increase in the RON of the isomerizate can only be got at the expense of the liquid yield.

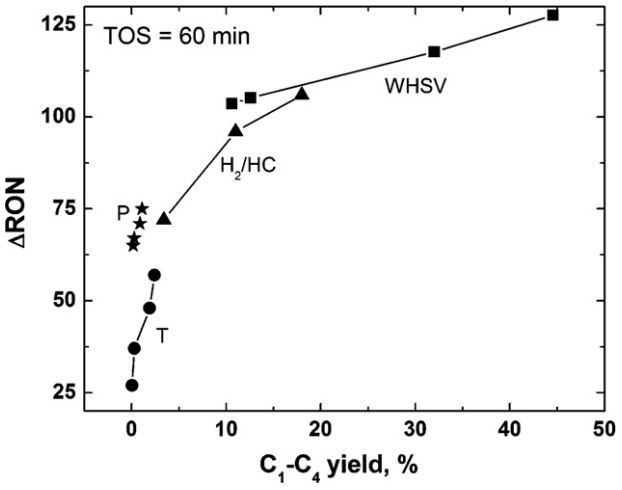

Fig. 11. RON gain as a function of yield of light gases.

When the H_2/HC and the WHSV are fixed and the other variables are let to vary the yield of light gases is not practically affected and the RON gain increases at more drastic reaction conditions. Then from the point of view of the throughput and the quality best conditions are those of maximum pressure and temperature.

4. Conclusions

A screening of reaction conditions for the isomerization-cracking of n-hexadecane on the Pt/WZ catalyst was made. The objective was to adjust the molecular size and to increase the branching of the isomerizate while maximizing the liquid yield and getting a stable activity level. With respect to the calcination temperature the objective was to maximize the conversion level. The most active Pt/WZ catalyst is obtained by calcination at 800 °C. The optimum temperature coincides with the formation of WO_3 crystals that are supposed to be centers of creation of Brönsted acid sites in the presence of hydrogen.

With respect to the temperature of reaction and the total pressure a high yield to hexadecane branched isomers can be got at low temperatures and high pressures (15–20 atm). Space velocity and H_2/HC were studied with a focus on the liquid C_5 + yield and the stability. The best yield to naphtha highly branched products can be obtained with a WHSV of 18 h^{-1}. Total stability can be got at a H_2/HC ratio of 6.

The overall analysis of the results from the point of view of quality and throughput indicates that RON gain and yield to light gases are strictly inversely proportional if temperature and pressure are fixed and the other variables are let to vary in a wide range. In plain terms this shows that the quality of the isomerizate can only be improved at the expense of the liquid yield in these conditions. If conversely the temperature or the pressure are set free, then the best (RON gain)/(light gases yield) ratio is obtained at high temperatures and pressures.

Acknowledgements

This work was supported with the financial funding of CONICET (PIP 2010-684) and Universidad Nacional del Litoral (CAI+D 2009 II PI 60-296). The authors also thank MEL Chemicals for supplying commercial tungsten zirconia.

References

[1] API, in: T.E. Daubert, R.P. Danner (Eds.), API Technical Data Book – Petroleum Refining, 6th edition, American Petroleum Institute (API), Washington, DC, 1997.
[2] V.M. Benitez, J.C. Yori, J.M. Grau, C.L. Pieck, C.R. Vera, Energy Fuels 20 (2006) 422–426.
[3] C.R. Vera, J.C. Yori, J.M. Parera, Appl. Catal. A 167 (1998) 75–84.
[4] X. Song, A. Sayari, Catal. Rev.-Sci. Eng. 38 (1996) 329–412.
[5] M. Hino, K. Arata, Catal. Lett. 30 (1995) 25–30.
[6] H. Deldari, Appl. Catal. A 293 (2005) 1–10.
[7] G. Wang, Q. Liu, W. Su, X. Li, Z. Jiang, X. Fang, C. Han, C. Li, Appl. Catal. A 335 (2008) 20–27.
[8] A. Martínez, G. Prieto, M.A. Arribas, P. Concepción, Appl. Catal. A 309 (2006) 224–236.
[9] J. Walendziewski, B. Pniak, B. Malinowska, Chem. Eng. J. 95 (2003) 113–121.
[10] T. Itoh, J. Mater. Sci. Lett. 5 (1986) 107–108.
[11] E.J. Mittemeijer, P. Scardi (Eds.), Diffraction Analysis of the Microstructure of Materials, vol. 68, Springer, Berlín, 2004.
[12] R.A. Young (Ed.), The Rietveld Method, vol. 5, Oxford University Press, New York, 1993.
[13] C.J. Howard, R.J. Hill, J. Mater. Sci. 26 (1991) 127–134.
[14] M. Boudart, Adv. Catal. Relat. Subjects 20 (1969) 158–160.
[15] G.A. Somorjai, Adv. Catal. 26 (1977) 56–58.
[16] N. Nikolaou, C.E. Papadopoulos, I.A. Gaglias, K.G. Pitarakis, Fuel 83 (2004) 517–523.

[17] M.A. Cortés-Jacome, C. Angeles-Chaveza, X. Bokhimib, J.A. Toledo-Antonio, J. Solid State Chem. 179 (2006) 2663–2673.
[18] J.C. Yori, C.L. Pieck, J.M. Parera, Appl. Catal. A: Gen. 181 (1999) 5–14.
[19] F. Babou, G. Coudurier, J.C. Vedrine, J. Catal. 152 (1995) 341–349.
[20] T. Lopez, J. Navarrete, R. Gomez, O. Novaro, F. Figueras, H. Armendariz, Appl. Catal. A 125 (1995) 217–232.
[21] G. Busca, Catal. Today 41 (1998) 191–206.
[22] J.R. Regalbuto, T.H. Fleish, E.E. Wolf, J. Catal. 107 (1987) 114–128.
[23] J.L. Contreras, G.A. Fuentes, Stud. Surf. Sci. Catal. 101 (1996) 1195–1204.
[24] B. Sen, M.A. Vannice, J. Catal. 113 (1988) 52–71.
[25] C. Hoang-Van, O. Zegaoui, Appl. Catal. A 130 (1995) 89–103.
[26] K. Shimizu, T.N. Venkatraman, W. Song, Appl. Catal. A 225 (2002) 33–41.
[27] C.D. Baertsch, K.T. Komala, Y.H. Chua, E. Iglesia, J. Catal. 205 (2002) 44–57.
[28] D.G. Barton, S.L. Soled, G.D. Meitzner, G.A. Fuentes, E. Iglesia, J. Catal. 181 (1999) 57–72.
[29] M. Busto, J.M. Grau, S. Canavese, C.R. Vera, Energy Fuels 23 (2009) 599–606.
[30] J.C. Parera, in: George J. Antos, Abdullah M. Aitani (Eds.), Catalytic Naphtha Reforming, 2nd edition, Marcel Dekker, 2004, p. 100.
[31] E. Iglesia, S.L. Soled, G.M. Kramer, J. Catal. 144 (1993) 238–253.
[32] R.A. Comelli, Z.R. Finelli, S.R. Vaudagna, N.S. Fígoli, Catal. Lett. 45 (1997) 227–231.
[33] J.-C. Duchet, D. Guillaume, A. Monnier, J. van Gestel, G. Szabo, P. Nascimento, S. Decaer, Chem. Commun. (1999) 1819–1820.
[34] J.C. Duchet, D. Guillaume, A. Monnier, C. Dujardin, J.P. Gilson, J. van Gestel, G. Szabo, P. Nascimento, J. Catal. 198 (2001) 328–337.
[35] K. Ebitani, J. Konishi, H. Hattori, J. Catal. 130 (1991) 257–267.
[36] K. Ebitani, J. Tsuji, H. Hattori, H. Kita, J. Catal. 135 (1992) 607–609.
[37] T. Shishido, H. Hattori, Appl. Catal. A 146 (1996) 157–164.
[38] T.N. Vu, J. van Gestel, J.P. Gilson, C. Collet, J.P. Dath, J.C. Duchet, J. Catal. 231 (2005) 468–479.
[39] M. Khurshid, S.S. Al-Khattaf, Appl. Catal. A 368 (2009) 56–64.
[40] M. Khurshid, M.A. Al-Daous, H. Hattori, S.S. Al-Khattaf, Appl. Catal. A 362 (2009) 75–81.
[41] Y. Sato, T. Hirose, F. Takahashi, M. Toda, Proc. 1st Pacific Chem. Eng. Congr., 1972, pp. 187–195.
[42] S. Fukushima, K. Kusaka, J. Chem. Eng. Jpn. 10 (1977) 461–468.
[43] M. Dudukovic, F. Larachi, P. Mills, Catal. Rev. 44 (2002) 123–246.
[44] M. Al-Dahhan, M. Dudukovic, Chem. Eng. Sci. 50 (1995) 2377–2389.
[45] Y. Wu, M. Khadilkar, M. Al-Dahhan, M. Dudukovic, A. Laurent, Eng. Chem. Res. 36 (1997) 3292–3314.
[46] M. Busto, S.A. d'Ippolito, J.C. Yori, M.E. Iturria, C.L. Pieck, J.M. Grau, C.R. Vera, Energy Fuels 20 (2006) 2642–2647.
[47] V.E. Sater, O. Levenspiel, Ind. Eng. Chem. Fundam. 5 (1966) 86–92.
[48] J.M. Hochman, E. Effron, Ind. Eng. Chem. Fundam. 8 (1969) 63–71.
[49] I.A. Furzer, R.W. Micell, AIChE J. 16 (1970) 380–385.
[50] R.W. Michell, I.A. Furzer, Chem. Eng. J. 4 (1972) 53–63.